An Enhanced Microgrid Load Demand Sharing Strategy

Jinwei He, *Student Member, IEEE*, and Yun Wei Li, *Senior Member, IEEE*

***Abstract*—For the operation of autonomous microgrids, an important task is to share the load demand using multiple distributed generation (DG) units. In order to realize satisfied power sharing without the communication between DG units, the voltage droop control and its different variations have been reported in the literature. However, in a low-voltage microgrid, due to the effects of nontrivial feeder impedance, the conventional droop control is subject to the real and reactive power coupling and steady-state reactive power sharing errors. Furthermore, complex microgrid configurations (looped or mesh networks) often make the reactive power sharing more challenging. To improve the reactive power sharing accuracy, this paper proposes an enhanced control strategy that estimates the reactive power control error through injecting small real power disturbances, which is activated by the low-bandwidth synchronization signals from the central controller. At the same time, a slow integration term for reactive power sharing error elimination is added to the conventional reactive power droop control. The proposed compensation method achieves accurate reactive power sharing at the steady state, just like the performance of real power sharing through frequency droop control. Simulation and experimental results validate the feasibility of the proposed method.**

***Index Terms*—Distributed generation (DG), droop control, low-bandwidth communication, microgrid, reactive power compensation, real and reactive power sharing.**

I. Introduction

THE application of distributed power generation has been increasing rapidly in the past decades. Compared to the conventional centralized power generation, distributed generation (DG) units deliver clean and renewable power close to the customer's end [1]. Therefore, it can alleviate the stress of many conventional transmission and distribution infrastructures. As most of the DG units are interfaced to the grid using power electronics converters, they have the opportunity to realize enhanced power generation through a flexible digital control of the power converters.

On the other hand, high penetration of power electronics-based DG units also introduces a few issues, such as system resonance, protection interference, etc. In order to overcome these problems, the microgrid concept has been proposed, which is realized through the control of multiple DG units. Compared to a single DG unit, the microgrid can achieve superior power management within its distribution networks. In addition, the islanding operation of microgrid offers high reliability power supply to the critical loads. Therefore, microgrid is considered to pave the way to the future smart grid [1].

In an islanded microgrid, the loads must be properly shared by multiple DG units. Conventionally, the frequency and voltage magnitude droop control is adopted, which aims to achieve microgrid power sharing in a decentralized manner [6], [11], [15]–[18], [20], [21]. However, the droop control governed microgrid is prone to have some power control stability problems when the DG feeders are mainly resistive [2]. It can also be seen that the real power sharing at the steady state is always accurate while the reactive power sharing is sensitive to the impacts of mismatched feeder impedance [3]–[5], [7]. Moreover, the existence of local loads and the networked microgrid configurations often further aggravate reactive power sharing problems [7], [18].

To solve the power control issues, a few improved methods have been proposed. In [1] and [2], the virtual frequency–voltage frame and virtual real and reactive power concept were developed, which improve the stability of the microgrid system. However, these methods cannot suppress the reactive power sharing errors at the same time. Additionally, when small synchronous generators are incorporated into the microgrid, proper power sharing between inverter-based DG units and electric machine-based DG units will be more challenging in these methods. In [3], both the reactive power and the harmonic power sharing errors were reduced with the noncharacteristic harmonic current injection. Although the power sharing problem was addressed, the corresponding steady-state voltage distortions degrade the microgrid power quality. In [4], a "Q–V dot droop" method was presented. It can be observed from [4] that the reactive power sharing improvement is not obvious when local loads are included. In [18], the reactive power sharing error reduction is realized using additional PCC voltage measurement. In [5]–[8], the predominant virtual output inductor is placed at the DG output terminal, which is mainly focused on preventing the power control instability. In addition, within the virtual impedance control frame, the reactive power sharing errors can be further reduced through an interesting model-based droop slope modification scheme [7]. As the virtual impedance aided control method has the ability to address the power control instability and power sharing errors at the same time, it is considered to be a promising way to provide superior microgrid performance [14]. However, it is worth mentioning that the aforementioned virtual

Manuscript received November 2, 2011; revised January 11, 2012; accepted February 24, 2012. Date of current version May 15, 2012. This paper was presented in part at the IEEE Energy Conversion Congress and Exposition-Asia (ECCE-Asia-2011), Jeju, Korea, 2011. Recommended for publication by Associate Editor Q.-C. Zhong.

The authors are with the Department of Electrical and Computer Engineering, University of Alberta, Edmonton, AB T6G 2V4, Canada (e-mail: hjinwei@ualberta.ca; yunwei.li@ualberta.ca).

Color versions of one or more of the figures in this paper are available online at http://ieeexplore.ieee.org.

Digital Object Identifier 10.1109/TPEL.2012.2190099

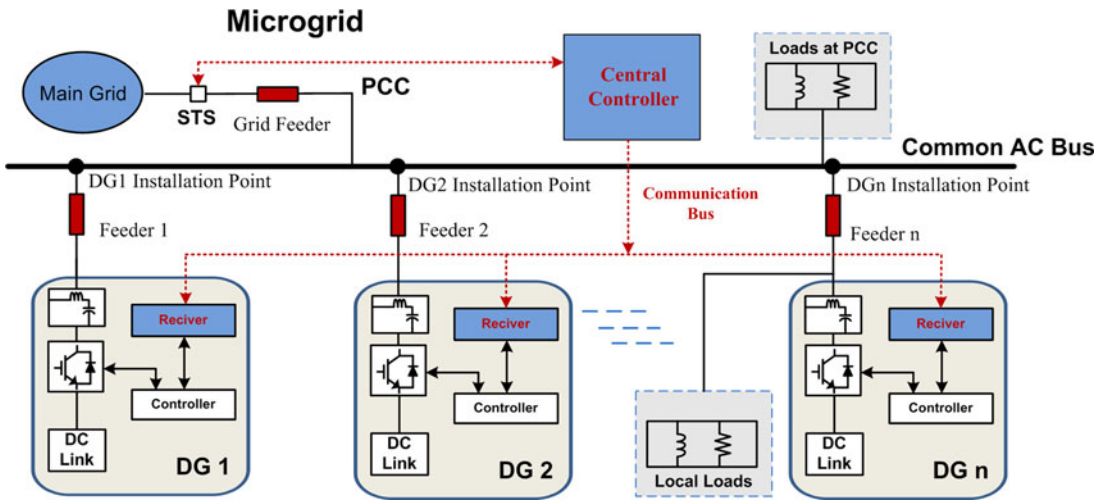

Fig. 1. Illustration of the microgrid configuration.

impedance control methods were developed based on simplified microgrid configurations. Indeed, due to the "plug-and-play" feature of DG units and loads [7], the microgrid configuration also changes with time. Without the real-time information of the microgrid configuration, virtual impedance control may not work properly as desired.

In response to the islanding microgrid control challenges, this paper presents a simple reactive power sharing compensation scheme. The proposed method first identifies the reactive power sharing errors through injecting small real-reactive power coupling disturbances, which are activated by the low-bandwidth synchronization flag signals from the central controller. Then the accurate reactive power sharing is realized by manipulating the injected transient real-reactive power coupling using an intermittent integral control. With the proposed scheme, reactive power sharing errors are significantly reduced. After the compensation, the proposed droop controller will be automatically switched back to the conventional droop controller. Note that the proposed accurate power control method is effective for microgrids with all types of configurations and load locations, and it does not need the detailed microgrid structural information. Simulation and experimental results are provided to verify the proposed load demand sharing method.

II. Analysis of the Conventional Droop Control Method

A. Operation of Microgrid

Fig. 1 illustrates the configuration of a microgrid. As shown, the microgrid is composed of a number of DG units and loads. Each DG unit is interfaced to the microgrid with an inverter, and the inverters are connected to the common ac bus through their respective feeders. Considering that the focus of this paper is the fundamental real and reactive power control, nonlinear loads are not considered in the microgrid. The microgrid and main grid status are monitored by the secondary central controller [14]. According to the operation requirements, the microgrid can be connected (grid-connected mode) or disconnected (islanding mode) from the main grid by controlling the static transfer switch (STS) at the point of common coupling (PCC). During the grid-connected operation, real and reactive power references are normally assigned by the central controller and the conventional droop control method can be used for power tracking. However, to eliminate the steady-state reactive power tracking errors, the PI regulation for the voltage magnitude control was developed in [7] and [11]. Therefore, power sharing is not a real concern during the grid-connected operation. When the microgrid is switched to islanding operation, the total load demand of the microgrid must be properly shared by these DG units.

During the islanding operation, DG units as illustrated in Fig. 1 can operate using the conventional real power–frequency droop control and reactive power–voltage magnitude droop control as

$$\omega = \omega_0 - D_P \cdot P \tag{1}$$

$$E = E_0 - D_Q \cdot Q \tag{2}$$

where ω_0 and E_0 are the nominal values of DG angular frequency and DG voltage magnitude, P and Q are the measured real and reactive powers after the first-order low-pass filtering (LPF), D_P and D_Q are the real and reactive power droop slopes. With the derived angular frequency and voltage magnitude in (1) and (2), the instantaneous voltage reference can be obtained accordingly.

B. Reactive Power Sharing Analysis

It is not straightforward to evaluate the reactive power sharing accuracy in a complex networked microgrid. For the sake of simplicity, this section first considers a simplified microgrid with two DG units at the same power rating. The configuration is shown in Fig. 2(a), where each DG unit has a local load. R_1 and X_1, and R_2 and X_2 are the feeder impedances of DG1 and DG2, respectively. Further considering that DG units are often equipped with series virtual inductors to ensure the stability of the system, the corresponding equivalent circuit is sketched in

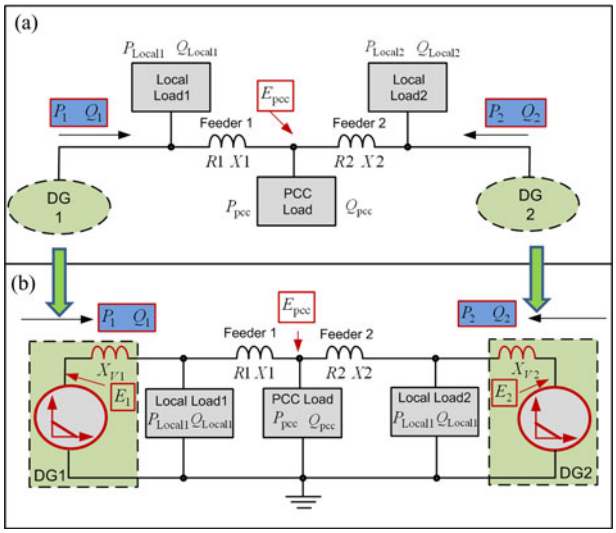

Fig. 2. Power flow in a simple microgrid: (a) configuration of the microgrid; (b) equivalent circuit model considering a virtual impedance control.

Fig. 2(b). As shown, the virtual reactances X_{V1} and X_{V2} are placed at the outputs of voltage sources. The magnitudes of the voltage sources are obtained in (3) and (4) as

$$E_1 = E_0 - D_Q \cdot Q_1 \tag{3}$$

$$E_2 = E_0 - D_Q \cdot Q_2 \tag{4}$$

where E_1 and E_2 are the DG voltage magnitudes regulated by the droop control, and Q_1 and Q_2 are the output reactive powers of DG1 and DG2, respectively.

For the power flowing through either physical or virtual impedance, its associated voltage drop on the impedance yields the following approximation as

$$\Delta V \approx \frac{X \cdot Q + R \cdot P}{E_0} \tag{5}$$

where P and Q are the real and reactive powers at the power sending end of the impedance, R and X are the corresponding resistive and inductive components of the impedance, E_0 is the nominal voltage magnitude, and ΔV is the voltage magnitude drop on the impedance.

Applying the voltage drop approximation in (5) to the presented system in Fig. 2(b), the relationships between DG voltages (E_1 and E_2) and the PCC voltage (E_{PCC}) can be established in (6) and (7) as

$$E_1 = E_{\mathrm{PCC}} + \frac{X_1 \cdot (Q_1 - Q_{\mathrm{Local1}}) + R_1 \cdot (P_1 - P_{\mathrm{Local1}})}{E_0} + \frac{X_{V1} \cdot Q_1}{E_0} \tag{6}$$

$$E_2 = E_{\mathrm{PCC}} + \frac{X_2 \cdot (Q_2 - Q_{\mathrm{Local2}}) + R_2 \cdot (P_2 - P_{\mathrm{Local2}})}{E_0} + \frac{X_{V2} \cdot Q_2}{E_0}. \tag{7}$$

It is important to note that with system frequency as the communication link, the real power sharing using the conventional droop control is always accurate [7]. Therefore, for the illustrated system at the steady state, the output real powers of DG1 and DG2 are obtained as

$$P_1 = P_2 = 0.5 \cdot P_{\mathrm{Total}} = 0.5 \cdot (P_{\mathrm{pcc}} + P_{\mathrm{Local1}} + P_{\mathrm{Local2}} + P_{\mathrm{Feeder1}} + P_{\mathrm{Feeder2}})$$

where P_{Total} means the real power demand within the islanded microgrid, and P_{Feeder1} and P_{Feeder2} are the real power loss on the feeders. Similarly, the reactive power demand (Q_{Total}) is defined as

$$Q_{\mathrm{Total}} = Q_{\mathrm{pcc}} + Q_{\mathrm{Local1}} + Q_{\mathrm{Local2}} + Q_{\mathrm{Feeder1}} + Q_{\mathrm{Feeder2}}$$

where Q_{Feeder1} and Q_{Feeder2} are the reactive power loss on the feeders.

By solving the obtained formulas from (3) to (7), the reactive power sharing error ($Q_1 - Q_2$) can be derived. The detailed expression is shown in (8), shown at the bottom of this page.

It can be noticed that the reactive power sharing error is related to a few factors, which include the offsets of local loads, unequal voltage drops on virtual and physical impedances, and the variations of the droop slope D_Q. When all these factors are considered at the same time, the evaluation of DG reactive sharing errors is not very straightforward even only two identical DG units are included in the analysis. Due to the complexity of the circuit model, the impacts of different factors shall be studied separately. For instance, the impacts of unequal feeder reactance to reactive power sharing error can be studied by ignoring the effects of local loads, feeder resistance, and virtual impedance. Fig. 3 demonstrates the reactive power sharing performance with mismatched feeder reactance, where the ideal inductive feeder leads to a linear relationship between the DG output reactive power and the magnitude difference between PCC voltage (E_{pcc}) and DG voltages (E_1 and E_2). The relationships are named as "DG1 feeder characteristics" and "DG2 feeder characteristics" in the figure. As shown, with mismatched feeder reactance ($X_1 < X_2$), the output reactive power of DG unit1 (Q_1) is higher than that of DG unit2 (Q_2) even the same droop slop (D_Q) is adopted for both DG units. It can also be observed that deeper droop slope D_Q^* might alleviate the reactive power sharing errors ($Q_1^* - Q_2^*$). However, the nontrivial feeder impedance may affect this error as well. Also, a deeper droop slope will cause many issues, such as a too low PCC

$$Q_1 - Q_2 = \frac{[(X_{V2} - X_{V1}) + (X_2 - X_1)] \cdot Q_{\mathrm{Total}} + (R_2 - R_1) P_{\mathrm{Total}} + 2[(X_1 Q_{\mathrm{Local1}} + R_1 P_{\mathrm{Local1}}) - (X_2 Q_{\mathrm{Local2}} + R_2 P_{\mathrm{Local2}})]}{X_{V1} + X_{V2} + X_1 + X_2 + 2D_Q \cdot E_0}. \tag{8}$$

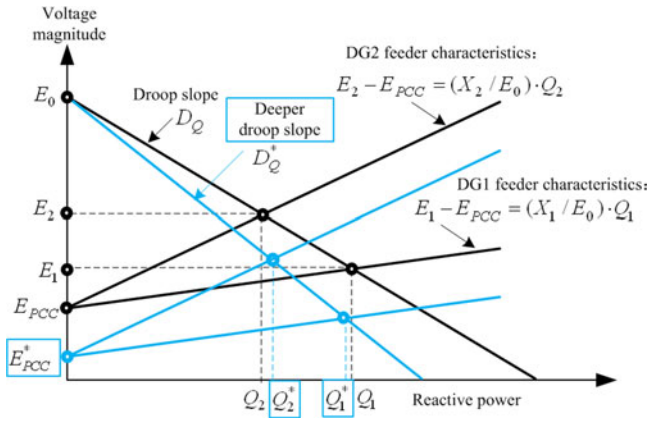

Fig. 3. Reactive power sharing of two DG units with mismatched feeder reactance.

voltage ($E^*_{\rm PCC}$), reactive power demand variations (due to voltage change), etc., and therefore, it is not considered as a good option [7].

III. Proposed Reactive Power Sharing Error Compensation Method

Since the reactive power sharing errors are caused by a number of factors and microgrids often have complex configurations, developing the circuit model-based reactive power sharing error compensation strategy is difficult. Therefore, the objective of this section is to develop an enhanced compensation method that can eliminate the reactive power sharing errors without knowing the detailed microgrid configuration. This feature is very important to achieve the "plug-and-play" operation of DG units and loads in the microgrid. To the best of the authors' knowledge, the accurate reactive power sharing method effective for complex networked microgrids has not been discussed in the literature so far.

A. Proposed Compensation Control

To initialize the compensation, the proposed method adopts a low-bandwidth communication link to connect the secondary central controller with DG local controllers [14]. The commutation link sends out the synchronized compensation flag signals from the central controller to each DG unit, so that all the DG units can start the compensation at the same time. This communication link is also responsible for sending the power reference for dispatchable DG units during the microgrid grid-tied operation. Therefore, the proposed compensation scheme does not need any additional hardware cost. The communication mechanism can be realized using power line signaling or smart metering technologies, or other commercial infrastructures, such as digital subscriber lines, or wireless communications. These techniques have already been suggested to construct the future smart grid systems in [20]. As the focus of this paper is the enhanced power sharing scheme realized at the DG unit local controller, further discussion on the communication system is out of the scope of this paper. Note that in the proposed compensation method, only one-way communication from the central controller to DG local controllers is needed for starting the DG compensation with a synchronized manner. The intercommunication among DG units is not necessary, so that the plug-and-play feature of a DG unit will not be affected.

The enhanced power control strategy is realized through the following two stages.

1) Stage 1: Initial Power Sharing Using Conventional Droop Method: Before receiving the compensation flag signal, the conventional droop controllers (1) and (2) are adopted for initial load power sharing. Meanwhile, the DG local controller monitors the status of the compensation flag dispatched from the microgrid central controller. During this stage, the steady-state averaged real power ($P_{\rm AVE}$) shall also be measured for use in *Stage 2*. Note that although the first-order LPFs have already been used in measuring the real and reactive powers (P and Q) for the conventional droop controller in (1) and (2), the cutoff frequency of LPFs cannot be made very low to get the ripple-free averaged real power ($P_{\rm AVE}$) due to the consideration of system stability [9], [21]. Therefore, a moving average filter is used here to further filter out the power ripples (see Fig. 4). The measured average real power ($P_{\rm AVE}$) is also saved in this stage, so that when the synchronization signal flag changes, the last saved value can be used for a reactive power sharing accuracy improvement control in *Stage 2*.

It is important to point out that although the averaged real power ($P_{\rm AVE}$) is measured at this stage, the real and reactive powers used in droop controller (1) and (2) are still conditioned by only first-order LPFs as shown in Fig. 4.

2) Stage 2: Power Sharing Improvement Through Synchronized Compensation: In *Stage 2*, the reactive power sharing error is compensated by introducing a real-reactive power coupling transient and using an integral voltage magnitude control term. As this compensation is based on the transient coupling power control, it shall be carried out in all DG units in a synchronized manner. Once a compensation starting signal (sent from the central controller) is received by the DG unit local controller, the averaged real power calculation stops updating, and the last calculated $P_{\rm AVE}$ is saved and used as an input of the compensation scheme. During the compensation process, the combination of both real and reactive powers is used in the frequency droop control as shown in (9), while the reactive power error is suppressed by using an additional integration term as illustrated in (10)

$$\omega = \omega_0 - (D_P \cdot P + D_Q \cdot Q) \tag{9}$$

$$E = E_0 - D_Q \cdot Q + \left(\frac{K_C}{s}\right) \cdot (P - P_{\rm AVE}) \tag{10}$$

where K_C is the integral gain, which is selected to be the same for all the DG units.

It can be observed that with the control strategy in (9), the real and reactive power is coupled together for the frequency droop control. Compared to the conventional droop control, the reactive power droop term ($D_Q \cdot Q$) in (9) can be considered as an offset for the conventional real power droop control for frequency regulation. If there are any reactive power errors, the unequal offsets ($D_Q \cdot Q$) from different DG units will affect

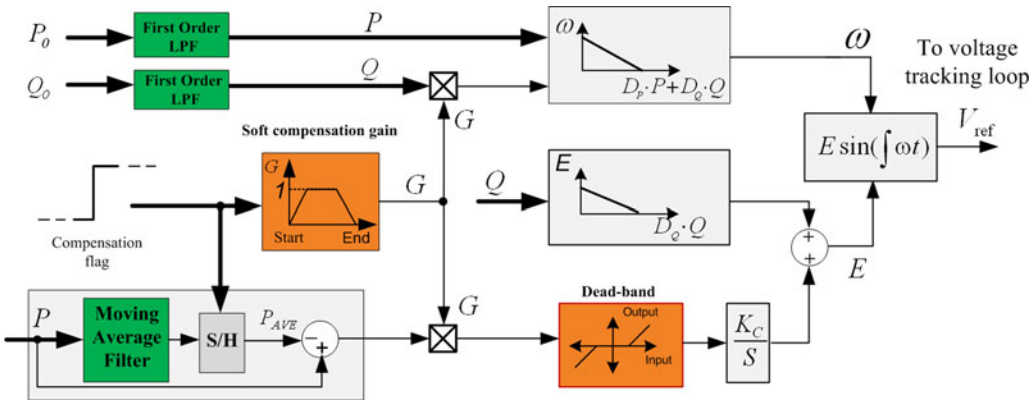

Fig. 4. Synchronized reactive power compensation scheme.

the DG output frequencies, which subsequently introduce the real power disturbances. This real power disturbance will then cause the integral control term in (10) to regulate the DG output voltage. With this integral control, the real power from a DG will eventually be equal to P_{AVE}, meaning that accurate real power sharing is still maintained in *Stage 2* (assume that there is no microgrid real power demand variations in the compensation period of *Stage 2*). Further consider that the modified frequency droop control in (9) essentially enables equal sharing of the combined power ($D_P \cdot P + D_Q \cdot Q$) in *Stage 2*; the accurate sharing of both the combined power and real power means that the reactive power sharing will also be accurate.

For instance, with the proposed control in (9), the DG units providing less reactive power in *Stage 1* will experience a transient real power increase in *Stage 2*. Therefore, an integration of the real power difference ($P-P_{\mathrm{AVE}}$) in a voltage magnitude control of (10) is able to eliminate the reactive power sharing error as discussed previously. Once the reactive power is shared properly, the DG unit real power flow will go back to its original value with the control of (9), and the integration control used in (10) will no longer contribute to the voltage magnitude regulation.

Fig. 4 demonstrates the diagram of the proposed control strategy, where P_0 and Q_0 are the measured powers before LPF. When the compensation is not enabled, the conventional power sharing method as shown in (1) and (2) is adopted. Once the compensation starts, the conventional control is replaced by (9) and (10). In Fig. 4, the unity soft compensation gain G is adopted for the proposed compensation method, which can avoid the excess power oscillations and current overshoots during the compensation transient. At the beginning of each compensation, the gain G will increase slowly to the rated value. After the compensation, G will decrease slowly to zero again, meaning that the droop controller is smoothly switched back to the conventional droop control mode.

The proposed method is developed based on the assumption that the real power load demand is constant during the compensation transient in *Stage 2*. For a real power load variation during the compensation stage, the proposed controller may leave some reactive power sharing errors after the compensation. There are two types of real power variations: steady-state real power variations/ripples and microgrid load switching. To limit the impacts of small real power demand variations during the compensation transient, a dead band is placed before the integral control of the real power difference ($P-P_{\mathrm{AVE}}$). To avoid the impacts of large load demand variations or load switching in a microgrid, the compensation period should be properly designed by tuning the integral gain (K_C) in (10). A long compensation period will subject to possible microgrid load demand changes, while a too fast compensation will lead to excess transient and affect the accuracy as well. Considering that the variation of microgrid load demand, such as that in the residential area microgrids, is normally slow [12], a compensation time of a few seconds in *Stage 2* is considered in this study.

A compensation dynamic of a few seconds also ensures that the compensation performance is not very sensitive to the "compensation flag" synchronization accuracy. Therefore, the requirements on the communication link bandwidth and the response time of DG unit local controllers can be quite low. For instance, even 0.1 s inconsistency of starting the compensation will not cause any obvious performance differences as will be shown in the next section. Furthermore, if the compensation function is activated in every few minutes/hours, the proposed method can always maintain an accurate reactive power sharing without affecting the power quality. This is different from the method in [3], where the noncharacteristic harmonic current is injected into the system continuously.

Finally, note that the soft compensation gain and the dead-band block are installed at the DG unit local controller. Also the compensation time (2 s in the simulations and experiments) is preset (by tuning the gain K_C) in the DG unit local controller and it is the same for all the DG units in the microgrid. Therefore, only the synchronized compensation start signals are required for the proposed controller. Any additional synchronized signals to terminate the compensation are unnecessary.

B. Small-Signal Modeling and Analysis

Compared to the conventional droop control, it can be seen that the renovated droop control method in (9) and (10) involves additional power couplings. In order to investigate the stability

and transient performances of DG units during the compensation process, small-signal analysis methods can be applied.

First, the power flow of the DG unit is obtained as

$$P = (EVY\cos(\theta) - V^2Y)\cdot\cos(\phi) - EVY\sin(\phi)\sin(\theta) \tag{11}$$

$$Q = (V^2Y - EVY\cos(\theta))\cdot\sin(\phi) - EVY\cos(\phi)\cos(\theta) \tag{12}$$

where P_0 and Q_0 are the instantaneous output powers of the DG unit; Y and Φ are the magnitude and angle of DG feeder admittance; E and V are the voltage magnitude at the DG unit output and the installation point, respectively. θ is the power angle.

Accordingly, real and reactive power variations according to DG voltage disturbances can be obtained in (13) and (14) as

$$\Delta P_0 = \left(\frac{\partial P_0}{\partial\theta}\right)\cdot\Delta\theta + \left(\frac{\partial P_0}{\partial E}\right)\cdot\Delta E = k_{P\theta}\cdot\Delta\theta + k_{PE}\cdot\Delta E \tag{13}$$

$$\Delta Q_0 = \left(\frac{\partial Q_0}{\partial\theta}\right)\cdot\Delta\theta + \left(\frac{\partial Q_0}{\partial E}\right)\cdot\Delta E = k_{Q\theta}\cdot\Delta\theta + k_{QE}\cdot\Delta E \tag{14}$$

where the operator Δ means small-signal disturbance around the DG system equilibrium point; $k_{p\theta}$, k_{pE}, $k_{Q\theta}$, and k_{QE} represent the power flow sensitivity to voltage angle and magnitude regulation.

When there are some power fluctuations during the compensation, by expanding the proposed compensation method in (9) and (10), the small-signal response of the DG voltage is expressed from (15) to (18) as

$$\Delta\omega = -D_P\cdot\Delta P - D_Q\cdot\Delta Q \tag{15}$$

$$\Delta E = -D_Q\cdot\Delta Q + \left(\frac{K_C}{s}\right)\cdot\Delta P \tag{16}$$

$$\Delta P = \frac{1}{(\tau s+1)}\cdot\Delta P_o \tag{17}$$

$$\Delta Q = \frac{1}{(\tau s+1)}\cdot\Delta Q_o \tag{18}$$

where τ is the time constant of LPFs used in the power calculation.

Considering that $\Delta\theta = (1/s)\cdot\Delta\omega$, by a simple manipulation on (13) to (18), the dynamic performance of the DG unit during the compensation yields the following matrix equation as

$$(A\,[2\times 2] - B\,[2\times 2]\cdot C[2\times 2])\cdot[\,\Delta\theta,\quad \Delta E\,]^T = 0 \tag{19}$$

where

$$A\,[2\times 2] = \begin{bmatrix} s(\tau s+1) & 0 \\ 0 & s(\tau s+1)\end{bmatrix}$$

$$B\,[2\times 2] = \begin{bmatrix} -D_P & -D_Q \\ K_C & -D_Q\cdot s\end{bmatrix}$$

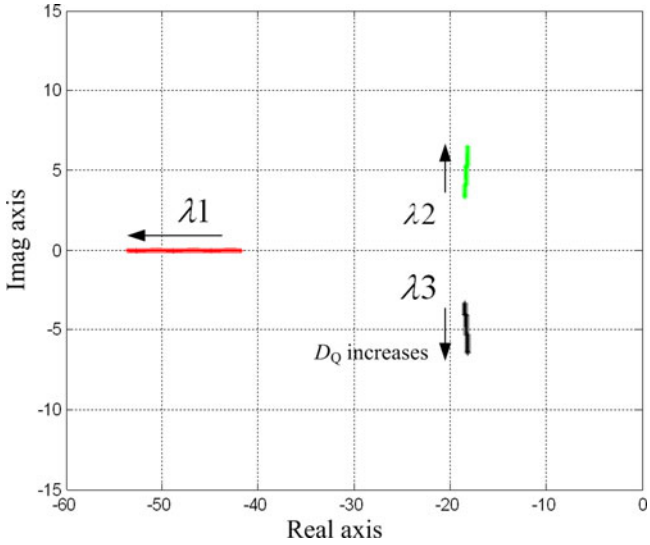

Fig. 5. Family of root locus diagram with the conventional droop controller: $D_P = 0.00145$, zero nondiagonal elements in $B[2\times 2]$, and $0.001 \le D_Q \le 0.00433$.

and

$$C\,[2\times 2] = \begin{bmatrix} k_{P\theta} & k_{PE} \\ k_{Q\theta} & k_{QE}\end{bmatrix}.$$

Furthermore, the closed-loop characteristic equation of the matrix equation can be obtained in

$$s^4\Delta\theta + As^3\Delta\theta + Bs^2\Delta\theta + Cs\Delta\theta + D = 0 \tag{20}$$

where *A, B, C,* and *D*, as shown in the equation at the bottom of the next page.

The eigenvalues of (19) and (20) indicate the small-signals response of the DG unit during the compensation. Note that when the nondiagonal elements of $B[2\times 2]$ are zero as

$$B\,[2\times 2] = \begin{bmatrix} -D_P & 0 \\ 0 & -D_Q\cdot s\end{bmatrix}$$

the corresponding matrix (19) essentially describes the behavior of the DG unit using the conventional droop control in (1) and (2).

The performances of the system with different control parameters are shown from Figs. 5–7. The DG unit circuit parameters are selected to be the same as in the simulation, and are listed in Table I. Fig. 5 shows the performance of the system using the conventional droop control method (corresponding to matrix $B[2\times 2]$ with zero nondiagonal elements), where the real power droop gain D_P is fixed while the reactive power droop slope D_Q increases from 0.001 to 0.00433. As illustrated, it is a three-order system and the dynamic performance of the system is mainly determined by the dominate poles λ_2 and λ_3. It can be seen that the positions of the dominate poles are not sensitive to the variations of reactive power droop slope within the given range.

During the compensation process, the response of the system to different reactive power droop slopes (D_Q) is also depicted in Fig. 6. In contrast to the conclusions from Fig. 5, the DG

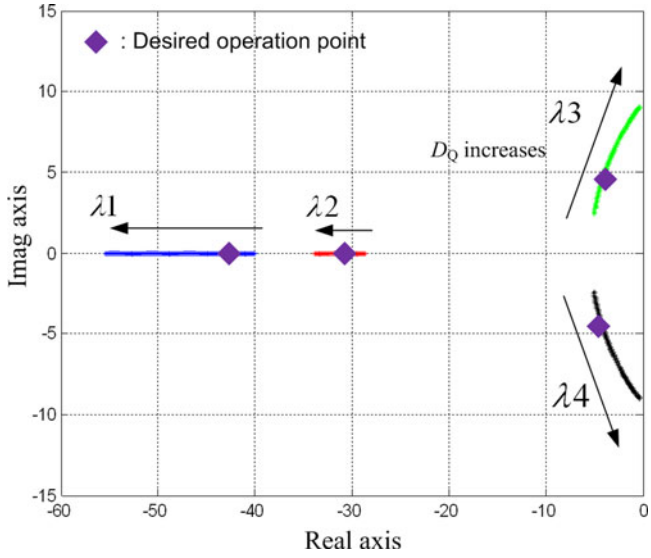

Fig. 6. Family of a root locus diagram with the proposed compensation controller: $D_P = 0.00145$, $K_C = 0.0286$, and $0.001 \leq D_Q \leq 0.00433$.

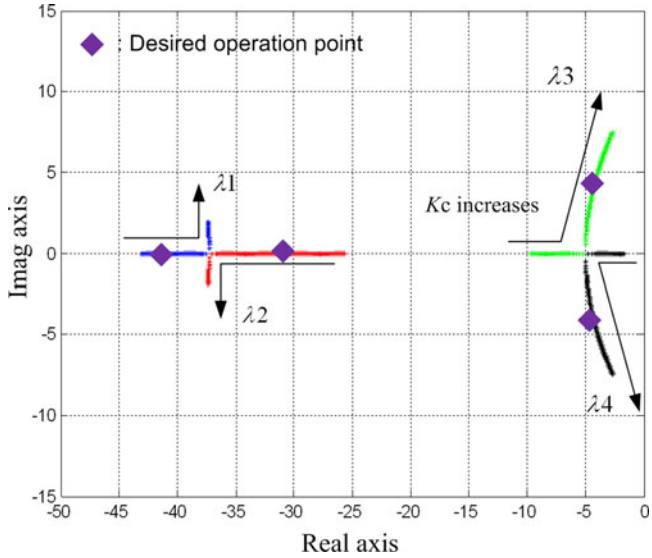

Fig. 7. Family of a root locus diagram with the proposed compensation controller: $D_P = 0.00145$, $D_Q = 0.00143$, and $0.01 \leq K_C \leq 0.05$.

unit becomes a fourth-order system in this case. Once again, the performance of system is evaluated by the dominate pole approximation. However, in this case, it can be observed that the performance of the system is more sensitive to the variation of D_Q within the same range. In order to obtain satisfied system damping and stability performance, the desired droop gain D_Q is selected as 0.0143.

Similarly, the response of the system to the integration gain (K_C) variations is examined in Fig. 7. It can also be observed that the stability and damping of the system is sensitive to change of the integration gain. To maintain proper stability and damping features, the selected gain K_C is 0.0286.

From the detailed small-signal analysis, it can be concluded that the stability and damping performance of the microgrid is affected during the compensation process. This phenomenon is very similar to the situation of reactive power tracking error elimination in the grid-connected mode, where the replacement of conventional reactive power droop controller with the PI controller makes the system performance more sensitive to the control parameter variations [8]. However, as will be demonstrated in the next section, the well-designed control parameter can maintain satisfied stability and damping performance during both steady-state operation and compensation transients.

IV. Simulation and Experiments

A. Simulation Verification

A networked microgrid model has been established using MATLAB/Simulink. As shown in Fig. 8, the simulated microgrid is composed of three identical DG units and two linear loads. With the same power rating, three DG units shall share the load equally. The detailed configuration of the DG unit is presented in Fig. 9, where an *LC* filter is placed between the IGBT bridge outputs and the DG feeders. The DG line current and filter capacitor voltage are measured to calculate the real and reactive powers. In addition, the well-known multiloop voltage controller is employed to track the reference voltage [7], [8] [14]. The circuit and control parameters of the DG unit are listed in Table I.

Fig. 10 demonstrates the reactive power flow of the DG units. Due to the unequal voltage drops on networked microgrid feeders, there are significant reactive power errors with the conventional droop control method. On the other hand, the proposed compensation method starting at 1.0 s can effectively adjust the reactive power sharing error to almost zero.

Fig. 11 shows the real power flow of these DG units. Before the compensation, the real power is evenly shared with the con-

$$A = \frac{\tau \cdot D_Q \cdot k_{QE} + 2\tau}{\tau^2}$$

$$B = \frac{-\tau \cdot K_C \cdot k_{PE} + D_Q \cdot k_{QE} + D_P \cdot k_{P\theta} \cdot \tau + D_Q \cdot k_{Q\theta} \cdot \tau + 1}{\tau^2}$$

$$C = \frac{D_Q \cdot k_{Q\theta} - D_P \cdot k_{PE} \cdot D_Q \cdot k_{Q\theta} - K_C \cdot k_{PE} + D_P \cdot k_{P\theta} + D_P \cdot k_{P\theta} \cdot D_Q \cdot k_{QE}}{\tau^2}$$

and

$$D = \frac{-D_Q \cdot k_{Q\theta} \cdot K_C \cdot k_{PE} \cdot D_Q \cdot k_{Q\theta} + D_Q \cdot k_{P\theta} \cdot K_C \cdot k_{QE}}{\tau^2}.$$

TABLE I
DG SYSTEM PARAMETERS

Parameter		*Values*
Interfaced Inverter (**Simulation& Experiment**)	Filter Inductor (L_f/R_f)	L:5mH/R:0.2Ω
	Filter Capacitor (C_f)	40uF
	Sampling-switching frequency	9kHz-4.5kHz
Microgrid Parameter (**Simulation**)	Rated RMS voltage (Line-Line)	208V (60Hz)
	Total Loads	3525W-1425Var
Droop coefficients (**Simulation**)	Frequency droop D_P	0.00125 Rad / (Sec • W)
	Voltage droop D_Q	0.00143 V/Var
	Integration dead-band	6 W
	Integral gain Kc	0.0286 V/ (Sec • W)
	LPF time constant τ	0.0159 Sec
Microgrid Parameter (**Experiment**)	Rated RMS voltage (Line-Line)	104V/60Hz
	Total Loads	540W/280Var
Droop coefficients (**Experiment**)	Frequency droop D_P	0.00143 Rad/(Sec • W)
	Voltage droop D_Q	0.00167 V/Var
	Integration dead-band	6 W
	Integral gain	0.0286 V/ (Sec • W)
	LPF time constant τ	0.0159 Sec

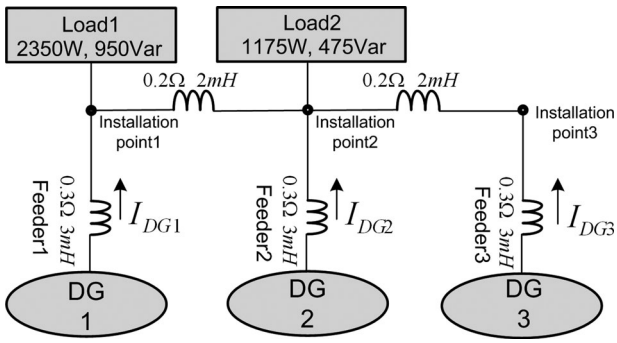

Fig. 8. Networked microgrid in the simulation.

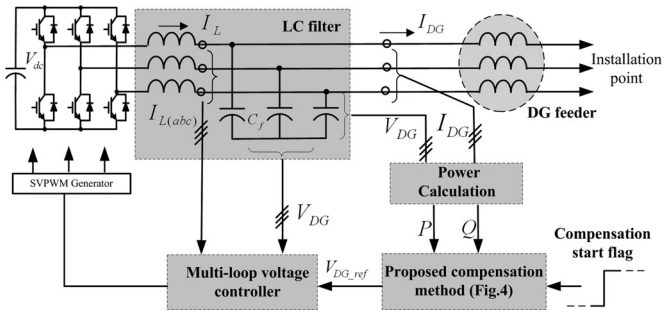

Fig. 9. Configuration of the DG unit.

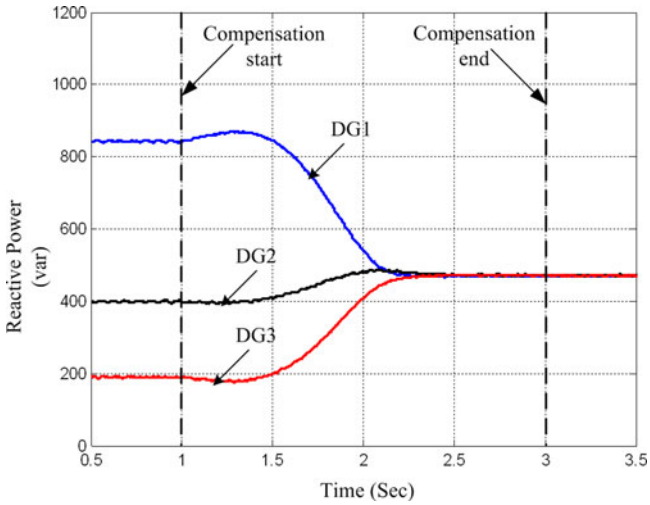

Fig. 10. Simulated reactive power sharing performance in a network microgrid (compensated is activated at 1 s).

ventional droop method. When the compensation is enabled at 1.0 s, due to the transient real and reactive power coupling introduced by (9) and (10), there are some disturbances in the real power. However, the output real power goes back to the original value at around 2.3 s.

Figs. 12 and 13 show the associated DG line currents. With the conventional droop control method, the magnitude and phase of DG currents are not the same as illustrated in Fig. 12. Consistent with the power sharing analysis, the DG line currents in Fig. 13 are almost identical after the compensation.

The voltage magnitudes at different locations of the microgrid are also obtained. Fig. 14 shows the changes of DG unit voltage magnitudes during this process. In order to realize equal reactive power sharing, these voltages have small deviations during the compensation. This is because the unequal voltage drops on the feeders are compensated by the DG units.

The voltage magnitudes at the installation points (see Fig. 8) are also obtained in Fig. 15. Similar to Fig. 14, these voltage magnitudes also have slight deviations during the compensation.

To test the sensitivity of the proposed compensated method to synchronization flag signal accuracy, a 0.1-s delay is intentionally added to the synchronization flag signal received by DG

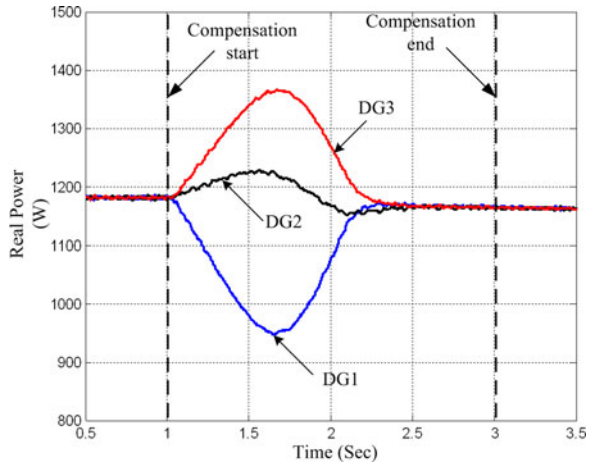

Fig. 11. Simulated real power sharing performance in a network microgrid (compensated is activated at 1 s).

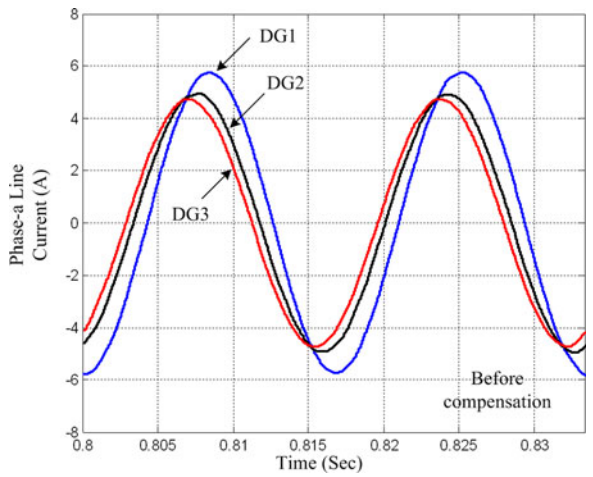

Fig. 12. Simulated DG currents before compensation.

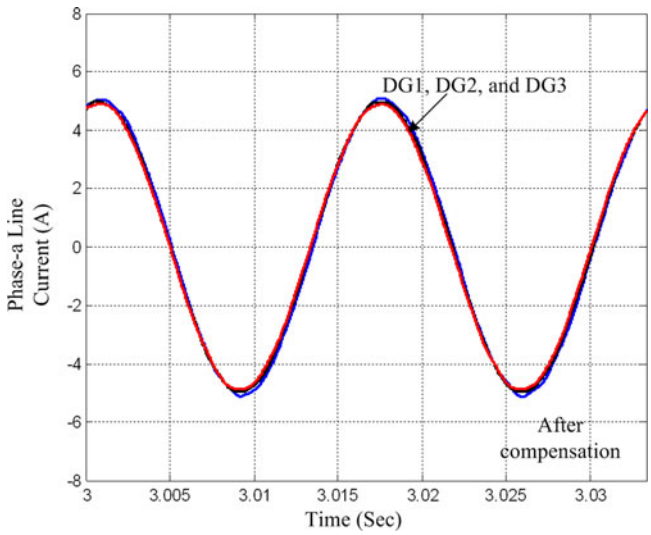

Fig. 13. Simulated DG currents after compensation.

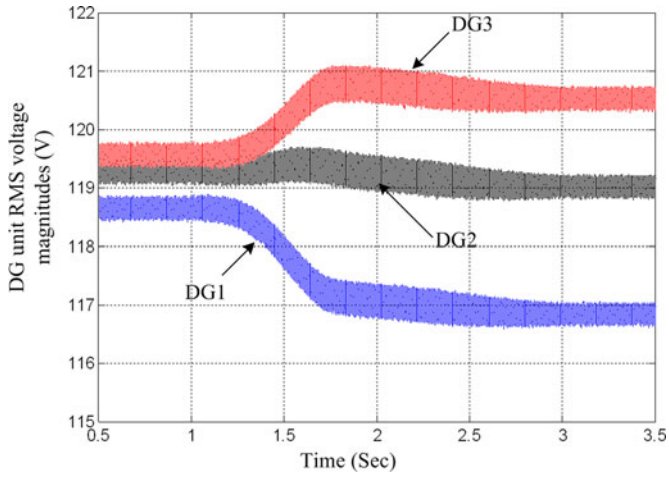

Fig. 14. Simulated DG voltage magnitudes.

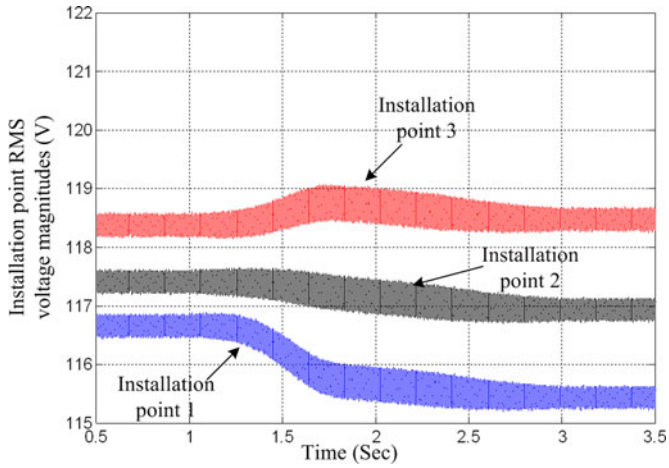

Fig. 15. Simulated installation points voltage magnitudes.

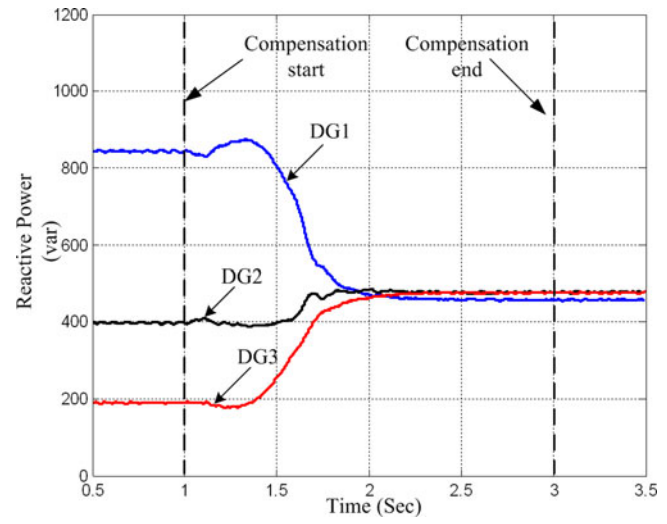

Fig. 16. Simulated reactive power sharing performance in a network microgrid (0.1 s synchronization flag delay in DG unit1).

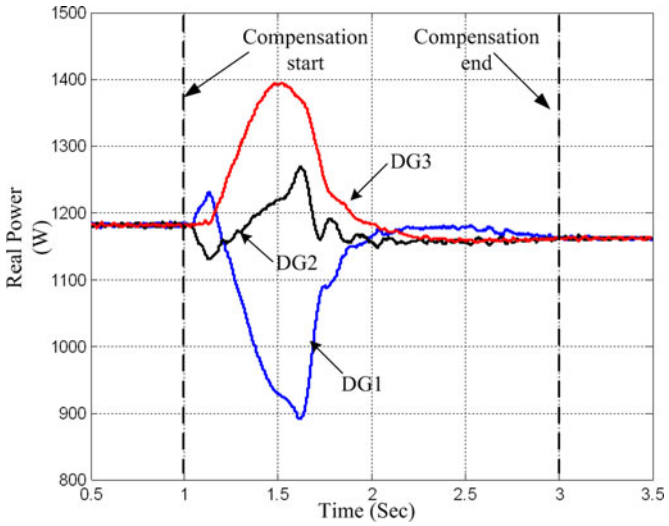

Fig. 17. Simulated real power sharing performance in a network microgrid (0.1 s synchronization flag delay in DG unit1).

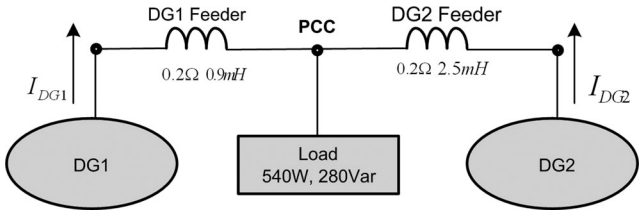

Fig. 18. Hardware microgrid in the experiment.

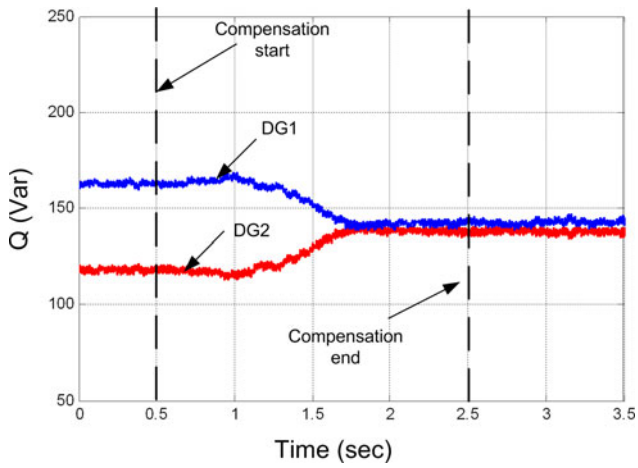

Fig. 19. Experimental reactive power sharing performance.

unit1, and the simulation results are shown in Figs. 16 and 17. Compared to the case in Figs. 10 and 11, it can be observed that the compensation performance is close to the situation without any delay. Although the reactive power sharing has very small steady-state errors after the compensation, the results are acceptable for most of the microgrid applications.

B. Experimental Verification

Experiments are conducted on a three-phase scaled microgrid prototype with two identical DG units. The system is controlled by the DSP (TMS2812)-FPGA system. The key parameters of the system are also listed in Table I. Once again, these two DG units shall share the load demand equally.

First, as shown in Fig. 18, two DG units are connected to a load with mismatched feeder impedances. The microgrid originally operates with the conventional droop control method. It can be

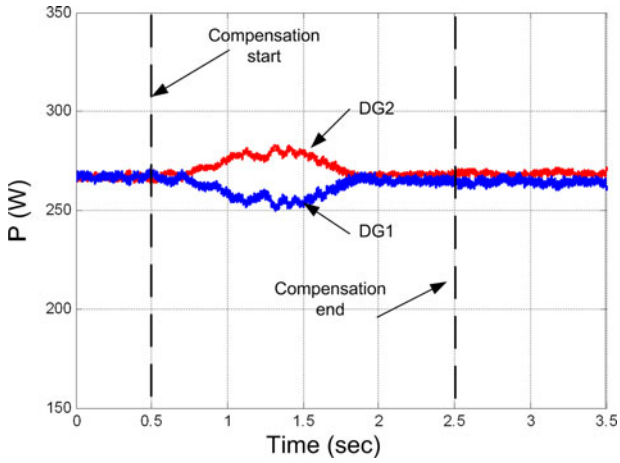

Fig. 20. Experimental real power sharing performance.

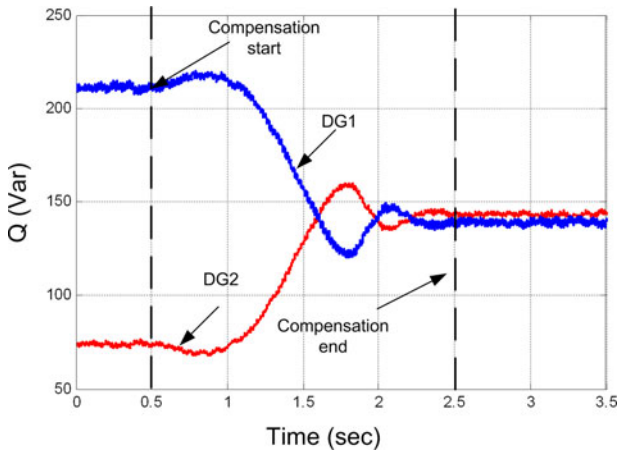

Fig. 21. Experimental reactive power sharing performance (bypass DG1 feeder impedance).

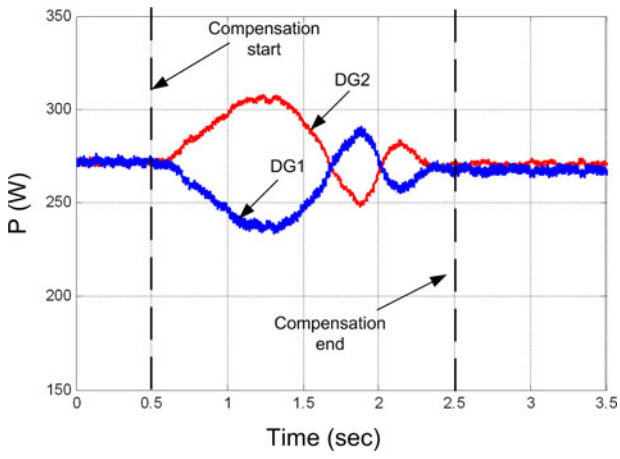

Fig. 22. Experimental real power sharing performance (bypass DG1 feeder impedance).

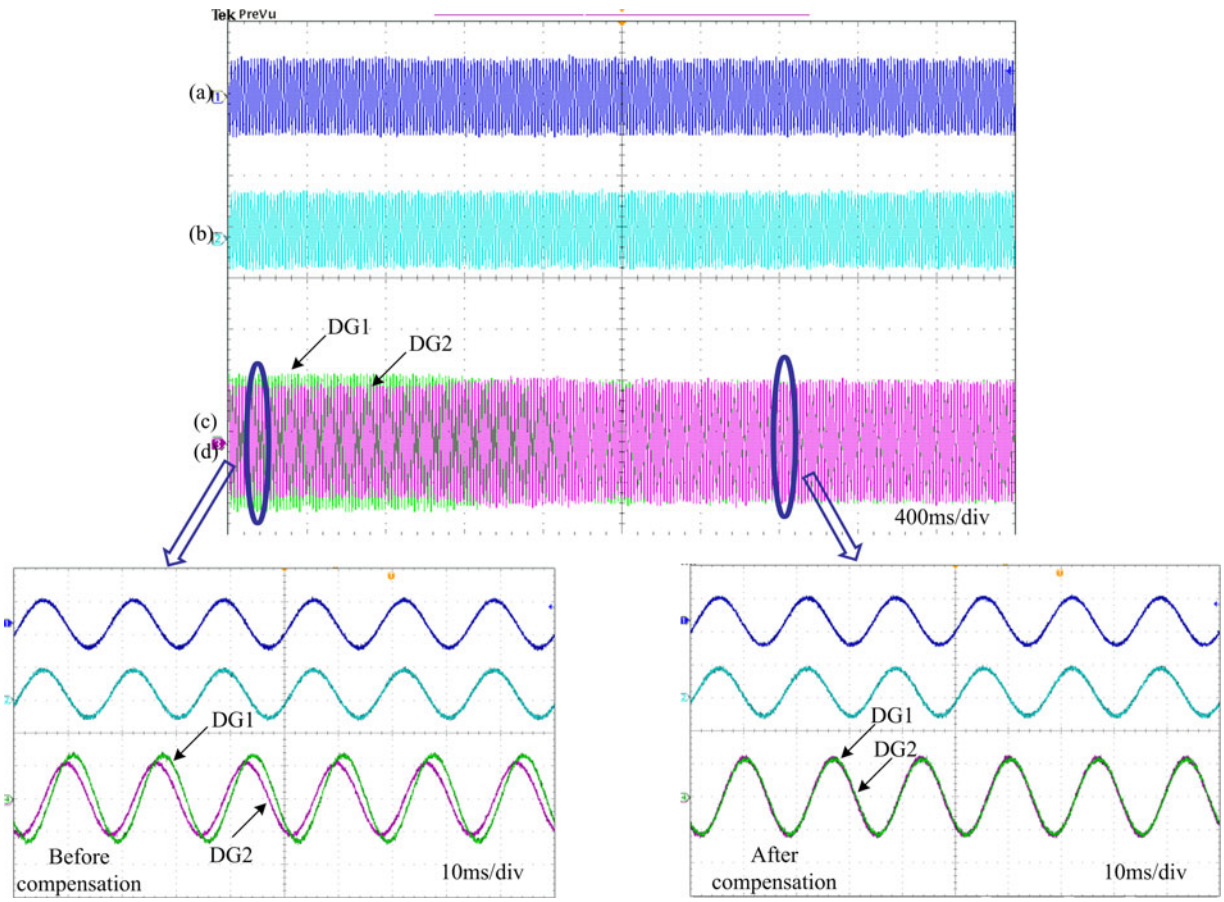

Fig. 23. DG current waveforms during the compensation. (a: DG1 voltage 200 v/div; b: DG2 voltage 200 v/div; c: DG1 current 2 A/div; d: DG2 current 2 A/div.)

seen that DG unit1 shares more reactive power as illustrated in Fig. 19, due to the effects of unequal feeder voltage drops. On the other hand, the real power sharing is accurate using the conventional droop control as shown in Fig. 20. When the proposed accurate power control is enabled at 0.5 s, the reactive power sharing accuracy in Fig. 19 is significantly improved. In addition, the stop of the proposed compensation scheme does not cause any obvious power oscillation.

To further verify the effectiveness of the compensation method, similar experiments are also conducted where the feeder impedance of DG unit1 reduces to zero. As can be seen from Figs. 21 and 22, the real power is equally shared with the conventional control while the majority of the reactive power is provided by DG1. As expected, an accurate reactive power sharing is achieved with the proposed compensation method.

The DG line current waveforms corresponding to Figs. 21 and 22 are obtained in Fig. 23. It can be seen that there is no obvious current overshoot during the whole compensation process and the line currents are always smooth. The zoom-in waveforms are shown in the lower part of the figure. As illustrated, due to the unequal feeder impedance, there is a significant current difference before the compensation. Consistent with the power control analysis, the current waveforms are almost identical after the compensation.

V. Conclusion

In this paper, an improved microgrid reactive power sharing strategy was proposed. The method injects a real-reactive power transient coupling term to identify the errors of reactive power sharing and then compensates the errors using a slow integral term for the DG voltage magnitude control. The compensation strategy also uses a low-bandwidth flag signal from the microgrid central controller to activate the compensation of all DG units in a synchronized manner. Therefore, accurate power sharing can be achieved while without any physical communications among DG units. In addition, the proposed method is not sensitive to microgrid configurations, which is especially suitable for a complex mesh or networked microgrid.

References

[1] A. Mehrizi-Sani and R. Iravani, "Potential-function based control of a microgrid in islanded and grid-connected modes," *IEEE Trans. Power Syst.*, vol. 25, no. 4, pp. 1883–1891, Nov. 2010.

[2] K. D. Brabandere, B. Bolsens, J. V. D. Keybus, A. Woyte, J. Drisen, and R. Belmans, "A voltage and frequency droop control method for parallel inverters," *IEEE Trans. Power Electron.*, vol. 22, no. 4, pp. 1107–1115, Jul. 2007.

[3] Y. Li and Y. W. Li, "Power management of inverter interfaced autonomous microgrid based on virtual frequency-voltage frame," *IEEE Trans. Smart Grid.*, vol. 2, no. 1, pp. 30–40, Mar. 2011.

[4] A. Tuladhar, H. Jin, T. Unger, and K. Mauch, "Control of parallel inverters in distributed AC power system with consideration of line impedance effect," *IEEE Trans. Ind. Appl.*, vol. 36, no. 1, pp. 131–138, Jan./Feb. 2000.
[5] C.-T. Lee, C.-C. Chu, and P.-T. Cheng, "A new droop control method for the autonomous operation of distributed energy resource interface converters," in *Proc. Conf. Rec. IEEE Energy Convers. Congr. Expo.*, Atlanta, GA, 2010, pp. 702–709.
[6] J. M. Guerrero, L. G. Vicuna, J. Matas, M. Castilla, and J. Miret, "Output impedance design of parallel-connected UPS inverters with wireless load sharing control," *IEEE Trans. Ind. Electron.*, vol. 52, no. 4, pp. 1126–1135, Aug. 2005.
[7] J. M. Guerrero, L. G. Vicuna, J. Matas, M. Castilla, and J. Miret, "A wireless controller to enhance dynamic performance of parallel inverters in distributed generation systems," *IEEE Trans. Power Electron.*, vol. 19, no. 4, pp. 1205–1213, Sep. 2004.
[8] Y. W. Li and C.-N. Kao, "An accurate power control strategy for power-electronics-interfaced distributed generation units operation in a low voltage multibus microgrid," *IEEE Trans. Power Electron.*, vol. 24, no. 12, pp. 2977–2988, Dec. 2009.
[9] J. He and Y. W. Li, "Analysis, design and implementation of virtual impedance for power electronics interfaced distributed generation," *IEEE Trans. Ind. Appl.*, vol. 47, no. 6, pp. 2525–2538, Nov./Dec. 2011.
[10] E. A. A. Coelho, P. C. Cortizo, and P. F. D. Garcia, "Small-signal stability for parallel-connected inverters in stand-alone AC supply systems," *IEEE Trans. Ind. Appl.*, vol. 38, no. 2, pp. 533–542, Mar./Apr. 2002.
[11] N. Pogaku, M. Prodanovic, and T. C. Green, "Modeling, analysis and testing of autonomous operation of an inverter-based microgrid," *IEEE Trans. Power Electron.*, vol. 22, no. 2, pp. 613–625, Mar. 2007.
[12] Y. W. Li, D. M. Vilathgamuwa, and P. C. Loh, "Design, analysis and real-time testing of a controller for multibus microgrid system," *IEEE Trans. Power Electron*, vol. 19, no. 5, pp. 1195–1204, Sep. 2004.
[13] J. A. Jardini, C. M. V. Tahan, M. R. Gouvea, S. U. Ahn, and F. M. Figueiredo, "Daily load profiles for residential, commercial and industrial low voltage consumers," *IEEE Trans. Power Del.*, vol. 15, no. 1, pp. 375–380, Jan. 2000.
[14] D. N. Zmood and D. G. Holmes, "Stationary frame current regulation of PWM inverters with zero steady-state error," *IEEE Trans. Power Electron.*, vol. 18, no. 3, pp. 814–822, May 2003.
[15] J. M. Guerrero, J. C. Vasquez, J. Matas, L. G. de Vicuna, and M. Castilla, "Hierarchical control of droop-controlled AC and DC microgrids—A general approach toward standardization," *IEEE Trans. Ind. Electron.*, vol. 55, no. 1, pp. 158–172, Jan. 2011.
[16] L. Corradini, P. Mattavelli, M. Corradin, and F. Polo, "Analysis of parallel operation of uninterruptible power supplies though long wiring cables," *IEEE Trans. Power Electron.*, vol. 25, no. 4, pp. 2806–2816, Apr. 2010.
[17] D. De and V. Ramanarayanan, "Decentralized parallel operation of inverters sharing unbalanced and nonlinear loads," *IEEE Trans. Power Electron.*, vol. 25, no. 12, pp. 3015–3025, Dec. 2010.
[18] P.-T. Cheng, C.-A. Chen, T.-L. Lee, and S.-Y. Kuo, "A cooperative imbalance compensation method for distributed generation interface converters," *IEEE Trans. Ind. Appl.*, vol. 45, no. 2, pp. 805–815, Mar./Apr. 2009.
[19] Q. Zhang, "Robust droop controller for accurate proportional load sharing among inverters operated in parallel," *IEEE Trans. Ind. Electron.*, to be published.
[20] J. He and Y. W. Li, "An accurate reactive power sharing control strategy for DG units in a microgrid," in *Proc. 8th Int. Conf. Power Electronics and ECCE Asia*, Jeju, Korea, 2011, pp. 551–556.
[21] V. Gungor, D. Sahin, T. Kocak, S. Ergut, C. Buccella, C. Cecati, and G. Hancke, "Smart grid technologies: Communications technologies and standards," *IEEE Trans. Ind. Inf.*, vol. 7, no. 4, pp. 529–539, Nov. 2011.
[22] E. A. A. Coelho, P. C. Cortizo, and P. F. D. Garcia, "Small signal stability for single phase inverter connected to stiff ac system," in *Proc. Conf. Rec. IEEE-IAS Annu. Meet.*, Oct. 1999, vol. 4, pp. 2180–2187.

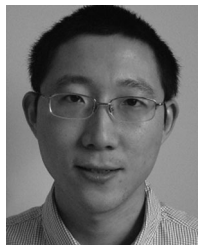

Jinwei He (S'10) received the B.Eng. degree from Southeast University, Nanjing, China, in 2005, and the M.Sc. degree from the Institute of Electrical Engineering, Chinese Academy of Sciences, Beijing, China, in 2008. He is currently working toward the Ph.D. degree from the University of Alberta, Edmonton, AB, Canada.

In 2007, he was a Visiting Student at the National Maglev Transportation Engineering R&D Center, Shanghai, China, where he was involved in the linear induction motor design project. From 2008 to 2009, he was with China Electronics Technology Group Corporation. He is the author or coauthor of more than 30 technical papers in refereed journals and conferences. His research interests include microgrid, distributed generation, and design, analysis, and control of linear electric machines.

Yun Wei Li (S'04–M'05–SM'11) received the B.Sc. degree in electrical engineering from Tianjin University, Tianjin, China, in 2002, and the Ph.D. degree from Nanyang Technological University, Nanyang, Singapore, in 2006.

In 2005, he was a Visiting Scholar with the Aalborg University, Aalborg, Denmark, where he was involved in the medium-voltage dynamic-voltage-restorer (DVR) system. From 2006 to 2007, he was a Postdoctoral Research Fellow at Ryerson University, ON, Canada, where he was involved in the high-power converter and electric drives. In 2007, he was also with Rockwell Automation, Inc., Canada, where he was responsible for the development of power factor compensation strategies for induction motor drives. Since 2007, he has been an Assistant Professor with the Department of Electrical and Computer Engineering, University of Alberta, Edmonton, AB, Canada. His research interests include distributed generation, microgrid, renewable energy, power quality, high-power converters, and electric motor drives.

Dr. Li serves as an Associate Editor for IEEE TRANSACTIONS ON INDUSTRIAL ELECTRONICS and a Guest Editor for the IEEE TRANSACTIONS ON INDUSTRIAL ELECTRONICS special session on distributed generation and microgrids.